

## The influence of temperature and thickness on the fracture behavior of P265GH material, using the J-integral method

Houda Salmi\*<sup>1)</sup>, Abdelilah Hachim<sup>2)</sup>, Hanan El Bhilat<sup>1)</sup> and Khalid El Had<sup>2)</sup>

<sup>1)</sup>Hassan II University of Casablanca (UH2C), National Higher School of Electricity and Mechanics (ENSEM), Laboratory of Control and Mechanical Characterization of Materials and Structures, Casablanca, Morocco

<sup>2)</sup>Heigher institute of maritims studies (ISEM), road d'El Jadida Casablanca- Morocco, ISEM, Km 7, laboratory of mechanics, Casablanca, Morocco

Received 30 May 2020  
Revised 26 October 2020  
Accepted 28 October 2020

### Abstract

In this work we examine, in elastoplastic case, the crack growth in P265GH material, we use eXtended finite element method (XFEM) in the Cast3m code. Crack growth in the 3D CT pipe sample is modeled using stress intensity factor and J integral. The comparison of the SIFs and the plastic zone size with analytical results validated the elasto-plastic numerical study; we analyzed the effect of loading and crack length on J integral. Finally, we analyzed the effect of both temperature and the specimen thickness on the fracture behavior of P265GH steel.

**Keywords:** P265GH Steel, Pressurized equipment, XFEM, Elastoplastic, Integral J, Temperature, Stress intensity factor

### 1. Introduction

In industrial sectors, pipelines have been used as the most economical and safest ways of transporting oil and gas. However, the number of accidents has increased considerably with the increasing number of their use, the design must take due account of all combinations possible of temperature and pressure that can produce reasonably foreseeable operating conditions of equipment.

Fracture is one of the most common forms of damage because the stress field at the crack tip takes the important values, this plays an important role in the determination of cracks initiation/propagation and it contributes to the creation of a plastic zone around the crack [1], therefore, it is important to know the exact size and shape of the plastic zone at the crack tip. The earliest theoretical work on the shape of the plastic zone was initiated by Irwin [2] and Dugdale [3]. Irwin estimated the extent of the plastic zone at the crack tip. Dugdale obtained the plastic zone from experimental tests on thin plates, the Dugdale model has been widely used to study plastic deformation near the crack tip.

In the elastic domain, the stress intensity factor is a robust parameter for the characterization of the crack growth but this notion is no longer valid in plasticity, for a constitutive law not linear, Rice and Rosengren [4] introduced the J integral as the variation of the potential energy during the crack propagation. They show that this energy release rate is independent of the integration contour surrounding the crack tip moreover its formulation is applied in the three-dimensional case.

The purpose of this study is to examine, in elastoplastic case, the three-dimensional crack growth for P265GH steel. For that, we used XFEM in the "Cast3M" code [5] and we worked on a 3D CT pipe sample:

We calculate the critical length of the crack leading to the fracture as well as the J integral.

We study the effect of the loading and the length of the crack on the J integral, we analyzed also the effect of both temperature and the specimen thickness on the fracture behavior of P265GH Steel in elastic-plastic range.

### 2. Materials and numerical methods

#### 2.1 Material

The study considered the P265GH steel at room temperature, this material is specially used in pressure equipment, this material is supposed to be elastic-plastic with kinematic hardening, with the following properties: Young's modulus  $E=200000$  MPa, yield stress  $\sigma_e=320$  MPa, Poisson's ratio  $\nu=0.3$ , breaking stress  $\sigma_r=470$  MPa, the nominal stress  $f=148$  MPa.

Hardening modulus  $H=200000$  MPa.

Fields in the vicinity of the crack tip can be represented by the HRR solution (Hutchinson Rice Rosengren) [6]. In this solution, the law of behavior is of Ramberg-Osgood type:

$$\frac{\varepsilon}{\varepsilon_e} = \frac{\sigma}{\sigma_e} + \alpha \left( \frac{\sigma}{\sigma_e} \right)^{n+1} \quad (1)$$

$n$  is the coefficient of hardening,  $\sigma_e$  is the elastic limit,  $\varepsilon_e$  is the limit deformation.

The stress field is approached by the following asymptotic solution [4]

$$\sigma_{ij} = \sigma_e \left( \frac{EJ}{\alpha r I_n \sigma_e^2} \right)^{1/(n+1)} \sigma_{ij}(n, \theta) \quad (2)$$

\*Corresponding author.

Email address: houda.salmi111@gmail.com

doi: 10.14456/easr.2021.33

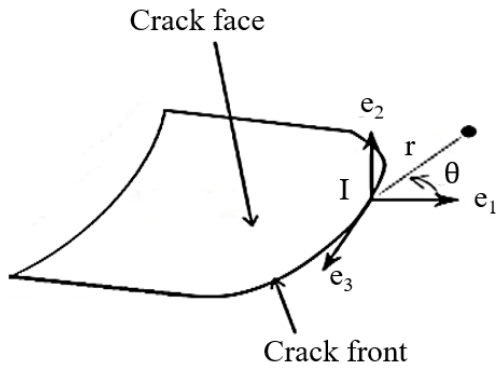


Figure 1 Local basis on the crack front

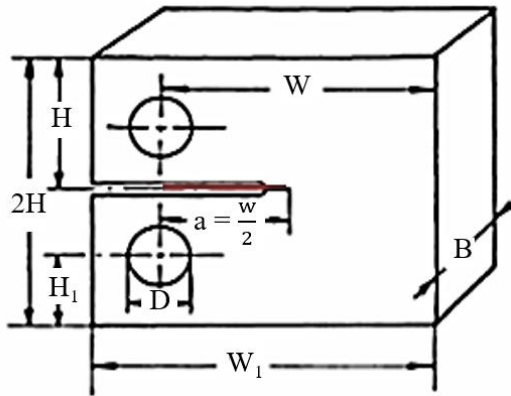


Figure 2 Dimension of the CT specimen

$$\varepsilon_{ij} = \frac{\alpha \sigma_e}{E} \left( \frac{EJ}{\alpha r I_n \sigma_e^2} \right)^{n/(n+1)} \varepsilon_{ij}(n, \theta) \quad (3)$$

Where  $I_n$  is an integration constant that depends on  $n$ ,  $\sigma_{ij}$  et  $\varepsilon_{ij}$  are tabulated functions of  $n$  and  $\theta$ .

For elastic-plastic behavior of a material with hardening effect, the J-integral can be expressed by Eq. (4) :

$$J = J_e(a_e) + J_p \quad (4)$$

Where  $J_e$  and  $J_p$  are respectively the elastic and plastic part of J.

$$J_e = \frac{K^2}{E'} \quad \text{with } E' = \frac{E}{(1-\nu^2)} \text{ in plane strain} \quad (5)$$

$$K = \sigma i_0 \sqrt{\pi a_e} \quad (6)$$

Where  $i_0$  is the elastic influence function for J-integral.

$a_e$  is the corrected crack depth in order to incorporate the effect of plastic deformation near the crack tip:

$$a_e = a + \frac{1}{\pi \beta} \left( \frac{K(a)}{\sigma_0} \right)^2 \quad (7)$$

with  $a$  is the crack depth,  $\beta = 2$  for plane stress, and  $\beta = 6$  for plane strain conditions.

2.2 J Integral in extended finite element method (XFEM)

The J-integral is the energy per unit fracture surface area, in a material [7], in this study, J is calculated by the G-Method (Eq. (8)), which is implemented in the software Castem [5]. Sukumar

[8] has used the gradient of the level sets to present the crack, [8] has defined this local basis by  $e_1 = \nabla \psi, e_2 = \nabla \varphi$  and  $e_3 = e_1 \wedge e_2$ .

In XFEM, J is expressed in a local basis formed of level set functions, J is given by Eq. (8) [8]:

$$J = \int_{\Gamma_c^+ \cup \Gamma_c^-} \theta_i P_{ij} n_j d\Gamma - \int_V \theta_i P_{ij} dV \quad (8)$$

Where  $P_{ij}$  is the Eshelby tensor [9], it is given by Eq.

$$P_{ij} = w \delta_{ij} - \sigma_{kj} \varepsilon_{ik} \quad (i, j, k) \in \{1, 2, 3\} \quad (9)$$

With  $w$  is the elastic energy density,  $\sigma$  and  $\varepsilon$  are respectively stress and strain expressed in the basis  $(e_1, e_2, e_3)$ .

$\theta$  is a field of displacement parallel to the plane of the crack and normal to the front Figure 1.

2.3 Geometry of study model and loading

We consider a sample CT from a pressurized pipe, the specimen contained a crack of an initial length  $a_0 = 11 \text{ mm}$  ( $a_0 / w = 0.55$ ), it is solicted in mode I by constant amplitude loading at 166 MPa. The value of the critical stress intensity is  $K_c = 96 \text{ MPa}\sqrt{\text{m}}$ , The dimensions of the CT specimen ( $W = 20 \text{ mm}, B = 10 \text{ mm}, w = 2. * B, a = 1.2 * B, f = 1.2 * B, u = 0.5 * B, W_1 = 2.5 * B, q = 0.65 * B$ ) are taken from the ASTM Standards [10] Figure 2.

$p$  is the value of internal pressure for the cylindrical shell, it is calculated according to the CODAP (C2.1.4.2) instructions [11]:

$$p = \frac{2 * \sigma_f * t * z}{D_m} \quad (10)$$

Where:

$D_m = 2. R_m = (R_i + R_e)$  is the mean radius of the pipe with circumferential crack,  $z$  is the welding coefficient, for an exceptional situation of service or resistance test,  $z = 1$ .

$t$  is the minimum thickness required of the cylindrical shell.

$\sigma_f$  is the applied stress in a pipe,  $\sigma_f$  equal to the nominal stress  $f$  for purely elastic behavior of the material.

For the elastic-plastic range, we choose  $\sigma_f \geq \sigma_e \gg f$ , with  $\sigma_e$  is the yield stress.

$(R_i$  and  $R_e)$  are respectively inner and outer radius of thin pipe. In this study, we use  $\sigma_f$  as applied loading.

2.4 Integration strategy and mesh of the CT specimen

To reproduce the crack advance, we defined the levels sets from a domain  $x$  Figure 3, the crack mesh Figure 4 as follow.

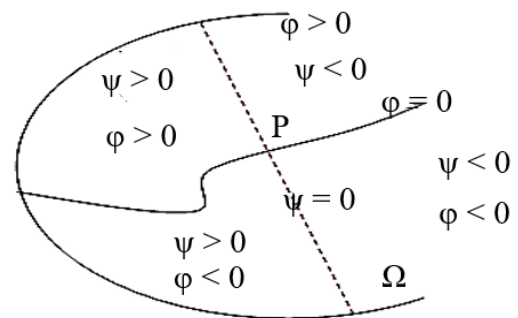


Figure 3 Representation of a crack with levels function

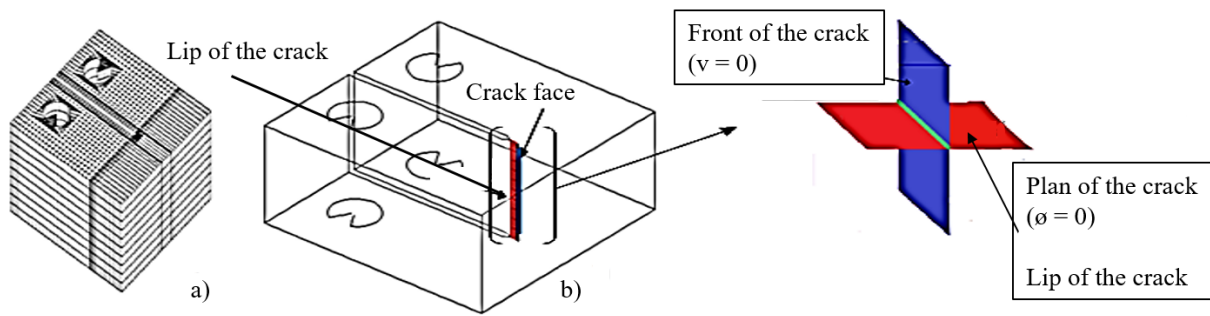


Figure 4 Simplification of definition of level set

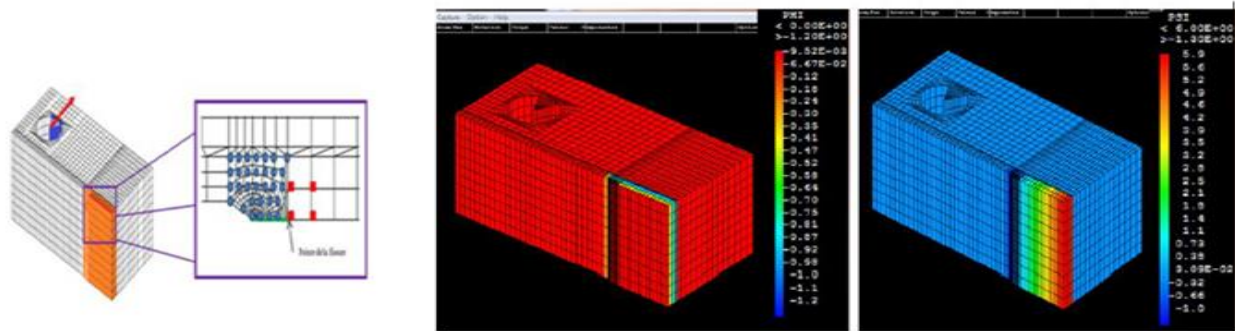


Figure 5 Zone of enrichment

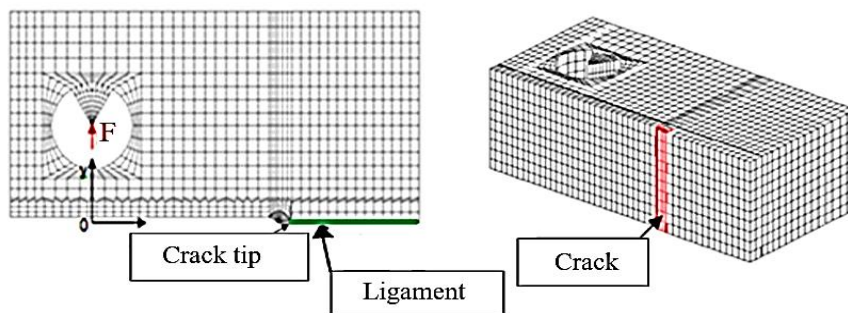


Figure 6 Loading and boundaries conditions

$$x \in \text{crack} \Rightarrow \begin{cases} \varphi(x) = 0 \\ \psi(x) \leq 0 \end{cases} \text{ with } (\nabla\psi = |\nabla\varphi| = 1) \quad (11)$$

The propagation is produced by extending the crack meshing by the numerical incrementation of its length  $a$ ; The new crack front can be deduced from the previous by a simple translation  $\Delta a$  such as  $a_{i+1} = a_i + \Delta a$ .

We modeled a half of CT specimen using 280 XFEM XC8R elements (orange, Figure 5).

Moreover, we used for the rest of mesh 10800 elements standard CUB8 (red, Figure 5) [12].

2.5 Loading and boundaries conditions

For the boundary conditions, the translation and the rotation according to the axes  $uy$  and  $uz$  are blocked. To ensure elastic deformation, we applied a low load  $\sigma_1 = 166\text{MPa}$  and  $\sigma_2 = 183\text{MPa}$ , then we increased the loading to  $\sigma = 330\text{MPa}$  to have the start of plastic zone near the crack tip.

The loading is applied on the CT specimen by means of a pin in the form of a rigid triangle to avoid any bending or parasitic torsion and to ensure that the tensile force is perfectly in the axis, the rigid triangle is indicated by the red arrow of the Figure 6.

3. Results and discussion

3.1 Numerical simulation in elastic case

The validation of the numerical study XFEM is done by comparison of the numeric values of SIF (Eq. (5)) with the analytical values (Eq. (12)) [13].

$$K = \frac{F}{B\sqrt{w}} [29,6 \left(\frac{a}{w}\right)^{1/2} - 185,5 \left(\frac{a}{w}\right)^{3/2} + 655,7 \left(\frac{a}{w}\right)^{5/2} - 1017 \left(\frac{a}{w}\right)^{7/2} + 638,9 \left(\frac{a}{w}\right)^{9/2}] \quad (12)$$

With  $F$ : the force applies in N,  $KI = SIF$ : stress intensity factor in mode I,  $\text{MPa}\sqrt{\text{m}}$ .  $a$ : the length of the crack, mm Figure 2.

Figures 7-8 presented the evolution of SIF calculated analytically and numerically by the two methods for the applied stresses  $\sigma_1 = 166\text{MPa}$  and  $\sigma_2 = 183\text{MPa}$ .

The relative error between the two numerical methods relative to the theory (Figure 9) is giving in Eq. (13)

$$e_{K1} = 100. \frac{(K_{ref} - K_{FEM})}{K_{ref}} \quad e_{K2} = 100. \frac{(K_{ref} - K_{XFEM})}{K_{ref}} \quad (13)$$

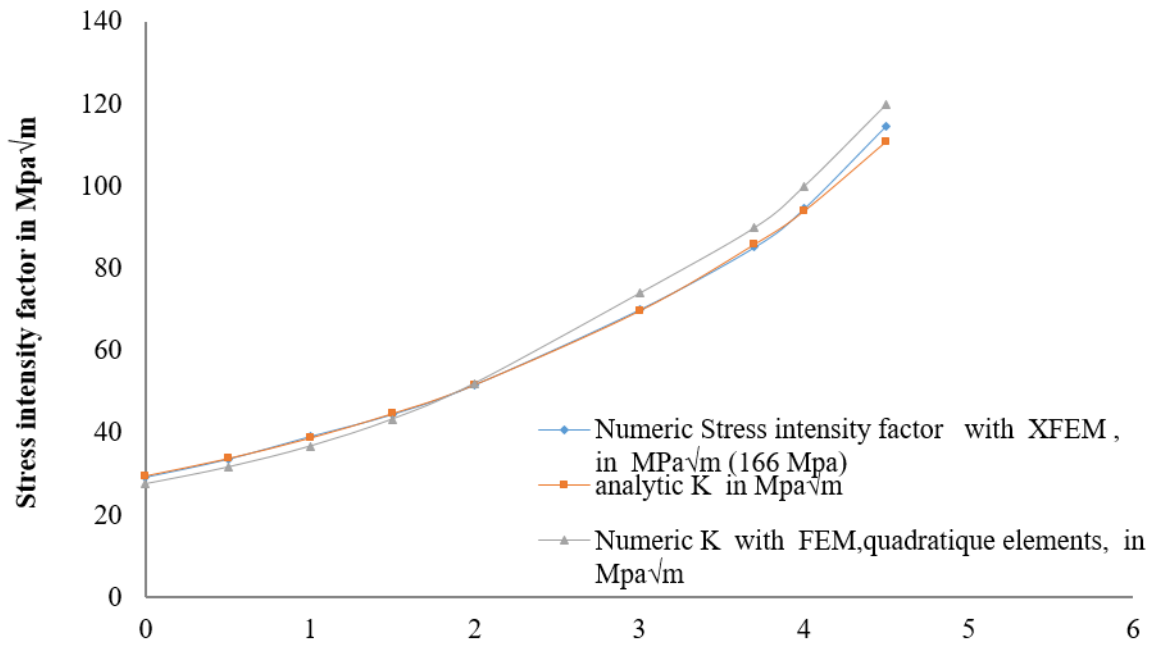


Figure 7 Evolution of SIF according to the progress of the crack da ( $\sigma = 166$  MPa)

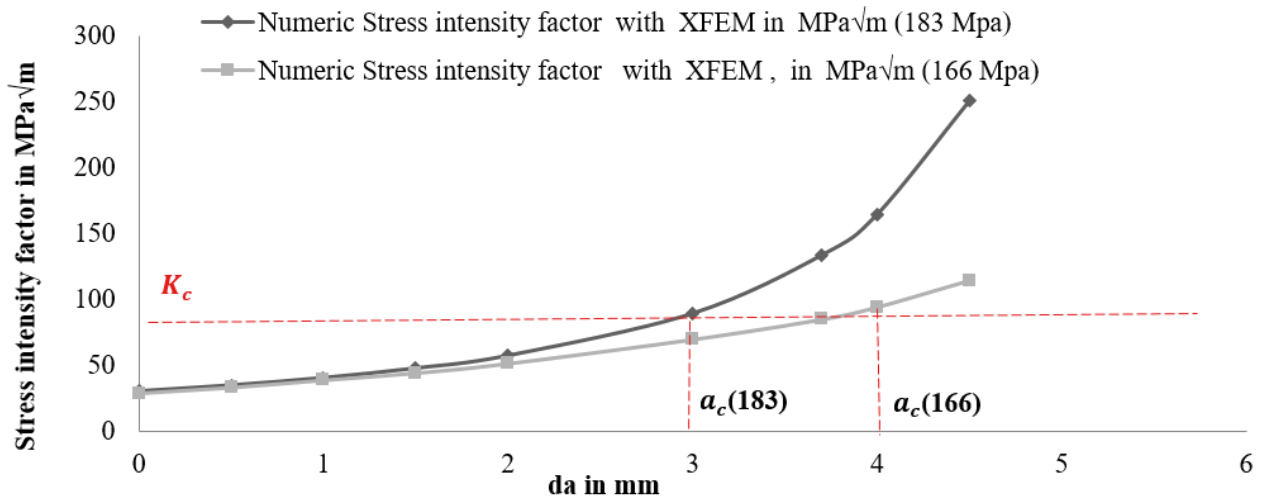


Figure 8 Evolution of SIF according to applied loading and the advanced crack

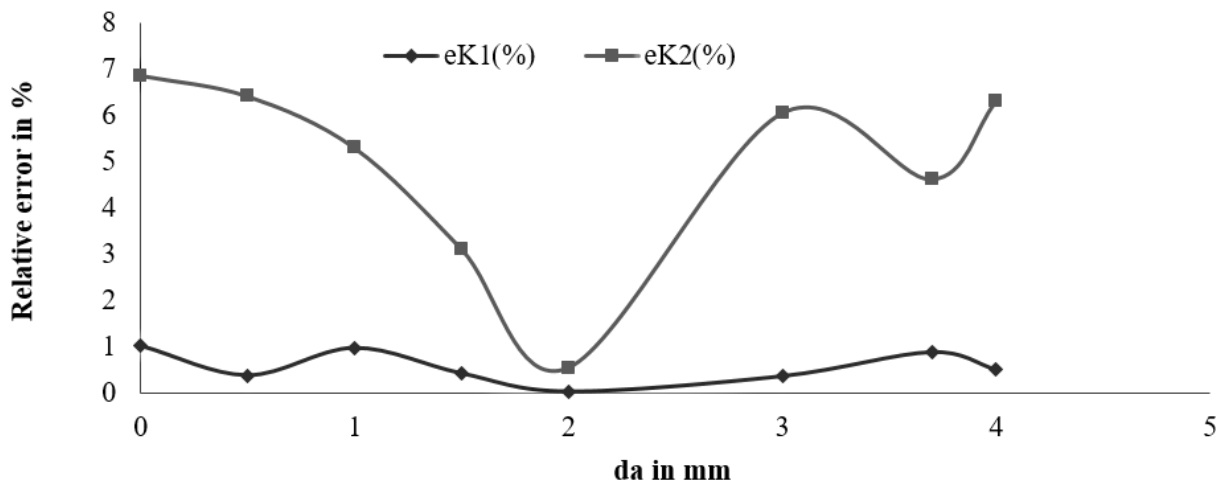


Figure 9 Relative error

Figures 7-8 Show that K increases when the crack light and loading values increase. The numerical values are comparable to the analytic with a relative error between 0% and 2% for XFEM so the XFEM is an accurate method [14-17], however for the simple geometry the FEM stay useful with a relative error between 1% et 8 % (Figure 9).

Figure 8 shows also that the value of the critical length of the crack advance is  $a_c = 4$  mm, moreover the value of the critical length of the crack leading to the break is related to the load, in fact below  $a_c$ , the crack propagates "slowly", in a gradual and stable manner, during loading; Once the critical size is reached, the crack propagates abruptly unstable, and very fast, which generally leads to rupture. The ductile material undergoes a large plastic deformation around the pre-cracked zone before breaking.

3.2 Numerical simulation in plastic case

The stress field at the crack tip is singular. It tends in theory towards infinity. In practice, this means that the threshold of plasticity at the crack tip is exceeded. The range of validity of the elastic approach is related to the size of the plastic zone created. As long as the plastic zone is weak relative to the ligament, the elastic domain is always valid, this is called confined plasticity (Figure 10), in this case, Irwin proposed a model for calculating the plastic zone in plane strain (Table 1. Eq (14)).

In the case where the size of the plastic zone becomes large relative to the ligament (extended plasticity); Dugdale-Barenblatt proposed a model that can be used both in confined and extended plasticity (Table 1. Eq (15)). Experimentally, the plasticity is confined [18] if:  $(w-a) > 2.5(\frac{K_C}{r_p})^2$  where  $(w-a)$  is the length of ligament (Figure 10).

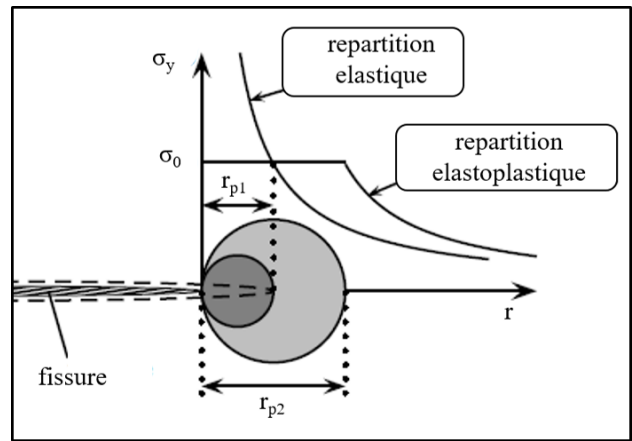


Figure 10 Plastic zone

Table 1 Analytical value of  $r_p$

Plastic zone size	Irwin model	Dugdale model
$r_p$	$\frac{1}{6\pi}(\frac{K_C}{\sigma_e})^2$ (14)	$A(\frac{1}{\cos(\frac{\pi\sigma}{2\sigma_e})} - 1)$ (15)
Analytical value of $r_p$ in our study	4 mm	3.5 mm

Table 1 shows that the Irwin model gives a value of  $r_p$  comparable with that given by the Dugdal model; for both analytical models we found that the size of the plastic zone  $r_p$  is comparable with the ligament ( $w-a = 20-7 = 13$  mm) therefore we are well in extended plasticity.

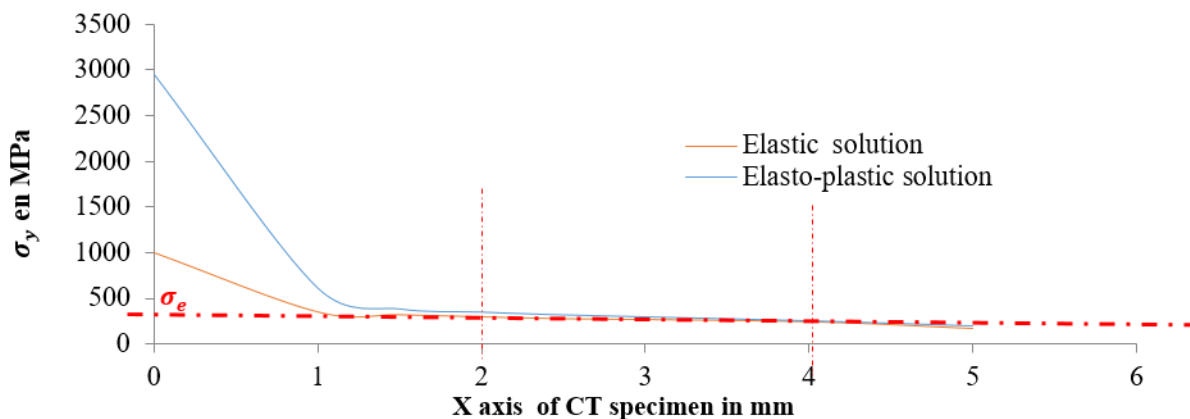


Figure 11 Stress field in crack tip

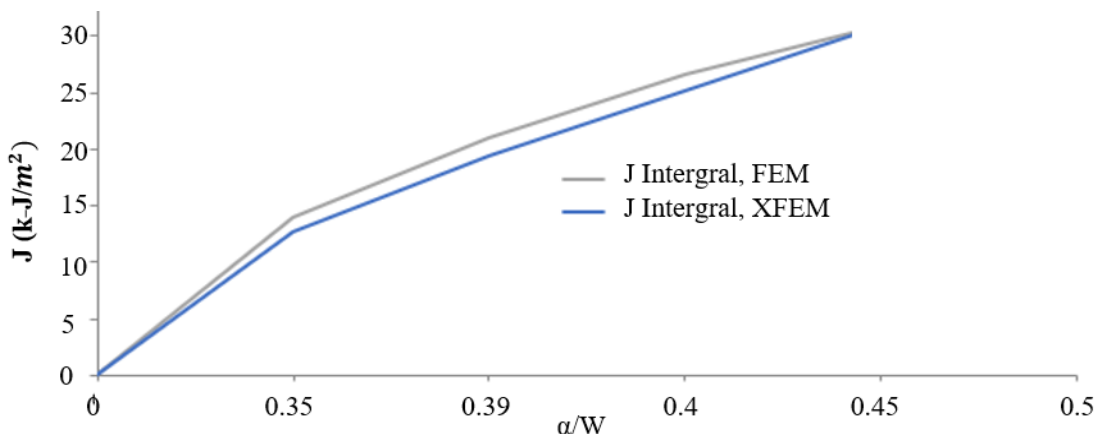
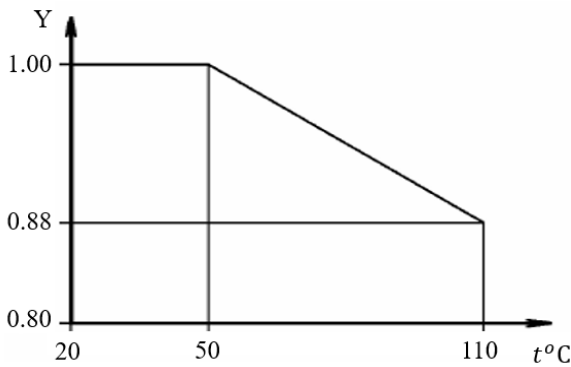


Figure 12 Evolution of the values of J integral according to crack advance,  $\sigma=330$  MPa,  $T=25$  °C.



**Figure 13** Mechanical characteristics at high temperature [11]

We calculated the  $r_p$  value numerically by Cast3M using XFEM:

From a crack length of  $2a = 14$  mm; We have traced the evolution of the normal stresses  $\sigma_y$  (Figure 11) along the x axis of the CT specimen (ligament, Figure 6), then we compared with the analytical results in Table 1.

Figure 11 shows that the maximum stress is focused at the crack tip, the numerical length of the plastic zone  $r_p$  in the elastoplastic behavior is  $r_{p2} = 4.2$  mm whereas in the elastic behavior  $r_{p1} = 2$  mm; So we verified the Irwin model where  $r_{p2} = 2 r_{p1}$ ;

Then the numerical results of  $r_p$  are comparable to the analytic values, which proves the numerical study with XFEM in elastoplastic case.

**3.3 The J integral**

We incremented numerically the crack length of a step of 1 mm, the initial length of the crack is 14 mm, we applied the loading  $\sigma = 330$  MPa.

Figure 12 shows that the values of J integral increases when the crack size increases, also the numerical values of J integral, calculated with FEM are comparable with the value given with FEM, which approve more the numerical study.

**3.4 The effect of temperature on J integral**

If the products are intended to be used at a temperature above ambient temperature, the corresponding characteristics must be defined by the product specification.

However, if the specification does not give the values of characteristics of hot traction, the value of the elastic limit to be taken into account for the calculation can be determined by the formula [11]:  $R_p^{t_{0.2}} = Y R_{p0.2} Y$  is given in Figure 13, which can only be used for a calculation temperature at most equal to 110° C.

Figure 14 presents the evolution of the value of J integral according to the crack advance and the temperature. The value of J integral increases when crack size and the value of temperature increase for  $T < 50$  °C the values of J integral are comparable, that to say at home temperature, the temperature doesn't influence the J integral. for  $T > 50$ °C, J integral is affected by the temperature and it attains his high value for a high value of temperature (110°C).

**3.5 The effect of thickness and temperature on J integral**

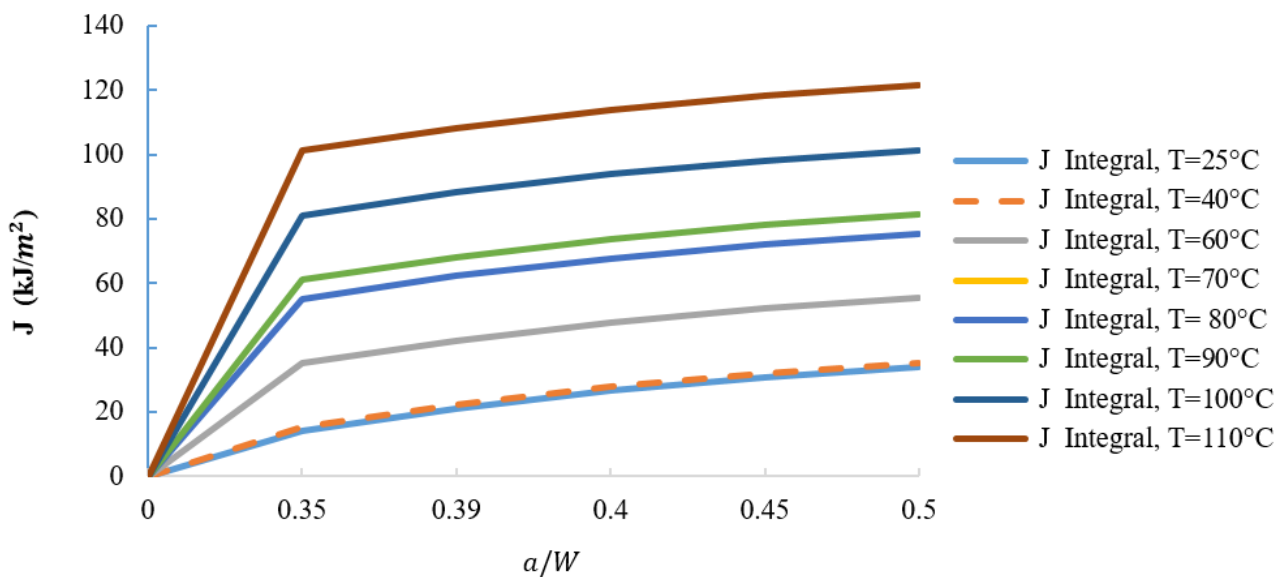
To know the effect of thickness on J integral, we varied the thickness and the temperature and presented the variation of J integral. Thickness takes the value 5, 7, and 10mm and the temperature is varied within the range 25 and 110 °C.

Figure 15 shows that the value of J integral decreases when the thickness of the specimen.

**4. Conclusion**

In this work XFEM is used to study, in elastic-plastic case, the three-dimensional crack growth for P265GH material, for that, we used the "Cast3M" code and we worked on a 3D CT pipe sample; The crack growth is modeled by the stress intensity factor in elastic case and the J contour integral in plastic case.

We checked the importance of the stress concentration at the crack tip, we have also determined the effect of temperature and the thickness on J integral values. The results show that the values of J integral increase when the load and the temperature increase, J integral decrease when the thickness increases, also the effect of temperature is noticeably remarkable on J integral for high values of temperature ( $T > 50$  °C).



**Figure 14** Evolution of J integral according the temperature and the crack advance.

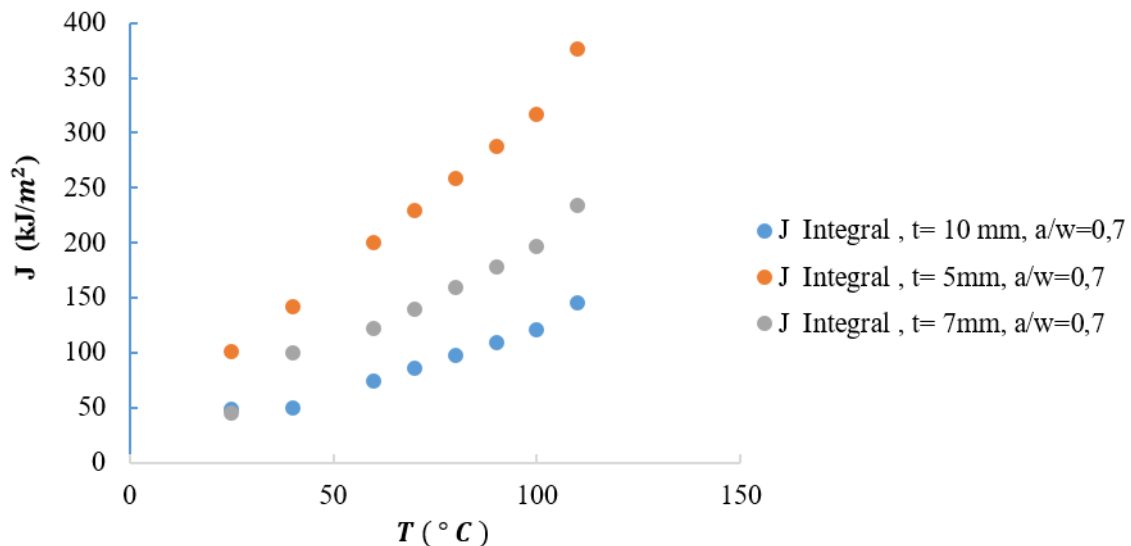


**Figure 15** Evolution of J integral according to the temperature and the thickness of the specimen.

## 5. References

- [1] Xin G, Wang H, Kang X, Jiang L. Analytic solutions to crack tip plastic zone under various loading conditions. *Eur J Mech Solid*. 2010;20:738-45.
- [2] Irwin GR. Plastic zone near a crack and fracture toughness. *Proceedings of the 7th Saga More Ordnance Materials Conference*. New York; 1960. p. 63-78.
- [3] Dugdale DS. Yielding of steel sheets containing slits. *J Mech Phys Solid*. 1969;9:100-6.
- [4] Rice JR, Rosengren GF. A path-independent integral and the approximate analysis of strain concentration by notches and cracks. *J Appl Mech*. 1980;35:379-86.
- [5] Le Fichoux E. *Présentation et utilisation de castem 2000*. 4<sup>th</sup> ed. ENSTA – LME: CEA; 1998.
- [6] Hutchinson JW. Singular behavior at the end of a tensile crack in a hardening material. *J Mech Phys Solid*. 1968;10:13-31.
- [7] Oommen B, Van Vliet KJ. Effects of nanoscale thickness and elastic nonlinearity on measured mechanical properties of polymeric films. *Thin Solid Films*. 2006;513:235-42.
- [8] Sukumar N, Chopp DL, Moran B. Extended finite element method and fast marching method for three-dimensional fatigue crack propagation. *Eng Fract Mech*. 2003;70:29-48.
- [9] Eshelby JD. The continuum theory of lattice defects. *Solid State Phys*. 1956;3:79-144.
- [10] Raheem Z. Standard test method for measurement of fracture toughness I. *Mater Sci*. 2019;1-56.
- [11] Gérard P, Alain B, Yves S, Frédéric L. CODAP, Code Français de Construction des Appareils à Pression non soumis à l'action de la flamme. 2005<sup>th</sup> ed. PARIS LA DÉFENSE CEDEX: SNCT; 2005. [In France].
- [12] Salmi H, El HK, El BH, Hachim A. Numerical study of SIF for a crack in P265GH steel by XFEM. In: Dos Santos S, Maslouhi M, Okoudjou K, editors. *Recent Advances in Mathematics and Technology*. Cham: Springer; 2020.
- [13] ASTM E1820-06. Standard test method for measurement of fracture toughness. Conshohocken: ASTM International; 2006.
- [14] Salmi H, Abdeliah H, Had KE, Bhilat HE. Numerical modeling and comparison study of elliptical cracks effect on pipes straight and with thickness transition exposed to internal pressure, using XFEM in elastic behavior. *J Comput Appl Res Mech Eng*. 2020;10(1):229-44.
- [15] Houada S, Khalid EH, Hanan EB, Abdelilah H. Numerical analysis of the effect of external circumferential elliptical cracks in transition thickness zone of pressurized pipes using XFEM. *J Appl Comput Mech*. 2019;5:861-74.
- [16] Bhilat HE, Had KE, Salmi, Hachim A. Thermo-mechanical characterization of post-consumer recycled high impact polystyrene from disposable cups: influence of the number of processing cycles. *J Comput Appl Res Mech Eng*. 2021;10(2):427-36.
- [17] Salmi H, Abdelilah H, Bhilat HE, Had KE. Crac influence on a pipe wiht double slope under internal pressure: numerical simulation with XFEM. *IJUM Eng J*. 2020;21(2):266-83.
- [18] Isabel D. *Nocivite d'un défaut semi-elliptique dans une coque fermee soumis a une pression interne*. France: University of Science and Technology of Lille; 1999.